Cell
Article

Supplemental figures

CellPress
OPEN ACCESS

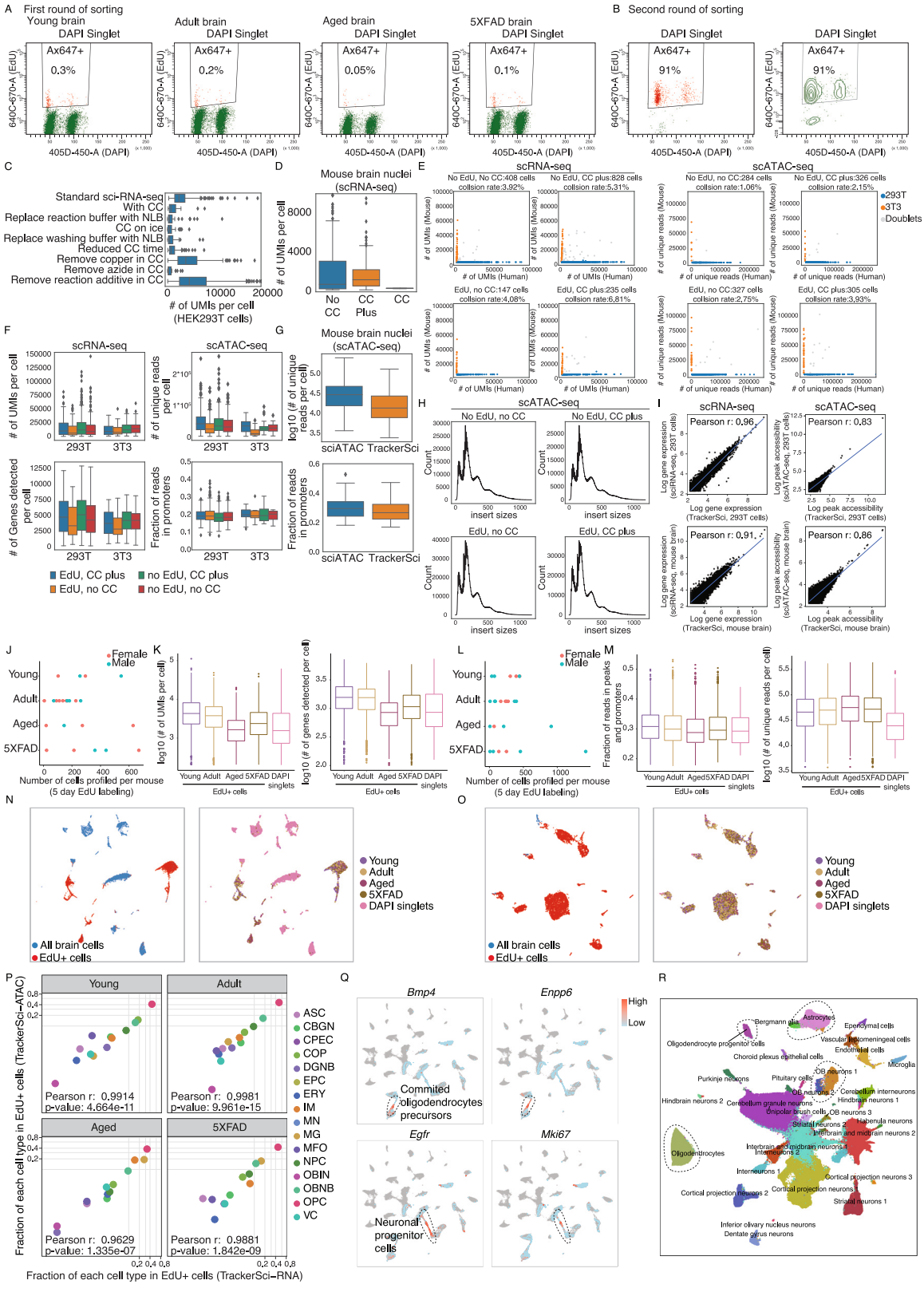

(legend on next page)

Figure S1. Quality control of *TrackerSci* for single-cell transcriptome and chromatin accessibility profiling for newborn cells, related to Figures 1 and 2

(A) Representative fluorescence-activated cell sorting (FACS) scatterplots showing the percentage of EdU+ cells in mouse brains across different conditions during the first round of sorting.

(B) FACS scatterplot (left) and contour plot (right) showing the percentage of EdU+ cells during the second round of sorting in *TrackerSci*.

(C) Boxplot showing the number of unique transcripts detected per cell (HEK293T nuclei) after different treatment conditions of click-chemistry (CC). The result indicated copper and reaction addictive in the conventional CC reaction decreased the scRNA-seq efficiency. NLB, nuclei lysis buffer. For all boxplots: middle lines, medians; upper and lower box edges, first and third quartiles, respectively; whiskers, 1.5 times the interquartile range; and diamonds are outliers.

(D) Boxplot showing the number of unique transcripts detected per cell (mouse brain nuclei) across three conditions: no click-chemistry (No CC), conventional click-chemistry (CC), and click-chemistry plus condition (with picolyl azide dye and copper protectant, CC Plus).

(E) Scatterplots showing the number of unique human and mouse transcripts (left)/reads (right) detected per cell across different conditions (with/without EdU labeling, with/without click-chemistry plus reaction). "No EdU, no CC" condition is representative of the traditional single-cell transcriptome/chromatin accessibility profiling.

(F) Boxplot showing the number of unique transcripts (top left) and genes (bottom left) from single-cell RNA-seq and the number of unique sequencing reads (top right) and the fraction of reads in promoters (bottom right) from single-cell ATAC-seq detected per cell in HEK293T and NIH/3T3 nuclei across the four conditions described in (E).

(G) Boxplots showing the number of unique ATAC-seq reads (top) and the fraction of reads in promoters (bottom) in mouse brain nuclei comparing traditional sci-ATAC-seq and *TrackerSci*.

(H) The aggregated fragment length distribution in ATAC-seq from *TrackerSci* of all cells across the four conditions described in (E).

(I) Scatterplot showing the correlation between log-transformed aggregated gene expression (transcripts per million, left) and ATAC-seq peak accessibility (reads per million, right) profiled by *TrackerSci* and conventional sci-RNA-seq/sci-ATAC-seq in HEK293T cells (top) and mouse brain cells (bottom), together with the linear regression line (blue).

(J) Scatterplots showing the number of single-cell transcriptomes profiled in each mouse individual across four conditions, colored by sexes. Only mice from the main experiment group (EdU labeling for 5 days) are shown.

(K) Boxplot showing the log-transformed number of unique transcripts (left) and genes (right) detected per cell profiled by *TrackerSci* and the DAPI singlet (without enrichment of EdU+ cells).

(L) UMAP visualization of single-cell transcriptomes, including EdU+ cells (profiled by *TrackerSci*) and all brain cells (without enrichment of EdU+ cells), colored by experiments (left) and conditions (right).

(M) Scatterplot showing the number of single-cell chromatin accessibility profiles in mouse individuals across four conditions, colored by sexes. Only mice from the main experiment group (EdU labeling for 5 days) are shown.

(N) Boxplot showing the fraction of reads in promoters and peaks (left) and the log-transformed number of unique ATAC-seq reads (right) detected per cell across different conditions in *TrackerSci* and the DAPI singlet (without enrichment of EdU+ cells).

(O) UMAP visualization of single-cell chromatin accessibility profiles, including EdU+ cells (profiled by *TrackerSci*) and all brain cells (without enrichment of EdU+ cells), colored by experiments (left) and conditions (right).

(P) Scatterplot showing the fraction of each cell type in the enriched EdU+ cell population by single-cell transcriptome (x axis) or chromatin accessibility analysis (y axis) in *TrackerSci* across different conditions. The Pearson correlation coefficients followed by a p value were added to the plot for each condition. ASC, astrocyte; CBGN, cerebellum granule neuron; CPEC, choroid plexus epithelial cell; COP, committed oligodendrocyte precursor; DGNB, dentate gyrus neuroblast; EPC, ependymal cell; ERY, erythroblast; IM, immune cell; MN, mature neuron; MG, microglia; MFO, myelin-forming oligodendrocyte; NPC, neuronal progenitor cell; OBIN, olfactory bulb inhibitory neuron; OBNB, olfactory bulb neuroblast; OPC, oligodendrocyte progenitor cell; VC, vascular cell.

(Q) UMAP visualization integrating the *TrackerSci* dataset and *EasySci* brain cell atlas, same as in Figure 2C. EdU+ cells profiled by *TrackerSci* are colored by markers for COPs (top) and NPCs (bottom), and the rest of cells are colored in gray.

(R) UMAP visualization of the full brain atlas dataset (~1.5 million cells) with the same parameter settings as in Figure 2C. Neurogenesis and oligodendrogenesis-related cell types are separated into distinct clusters, while the "bridge" cells in the intermediate stages are missing.

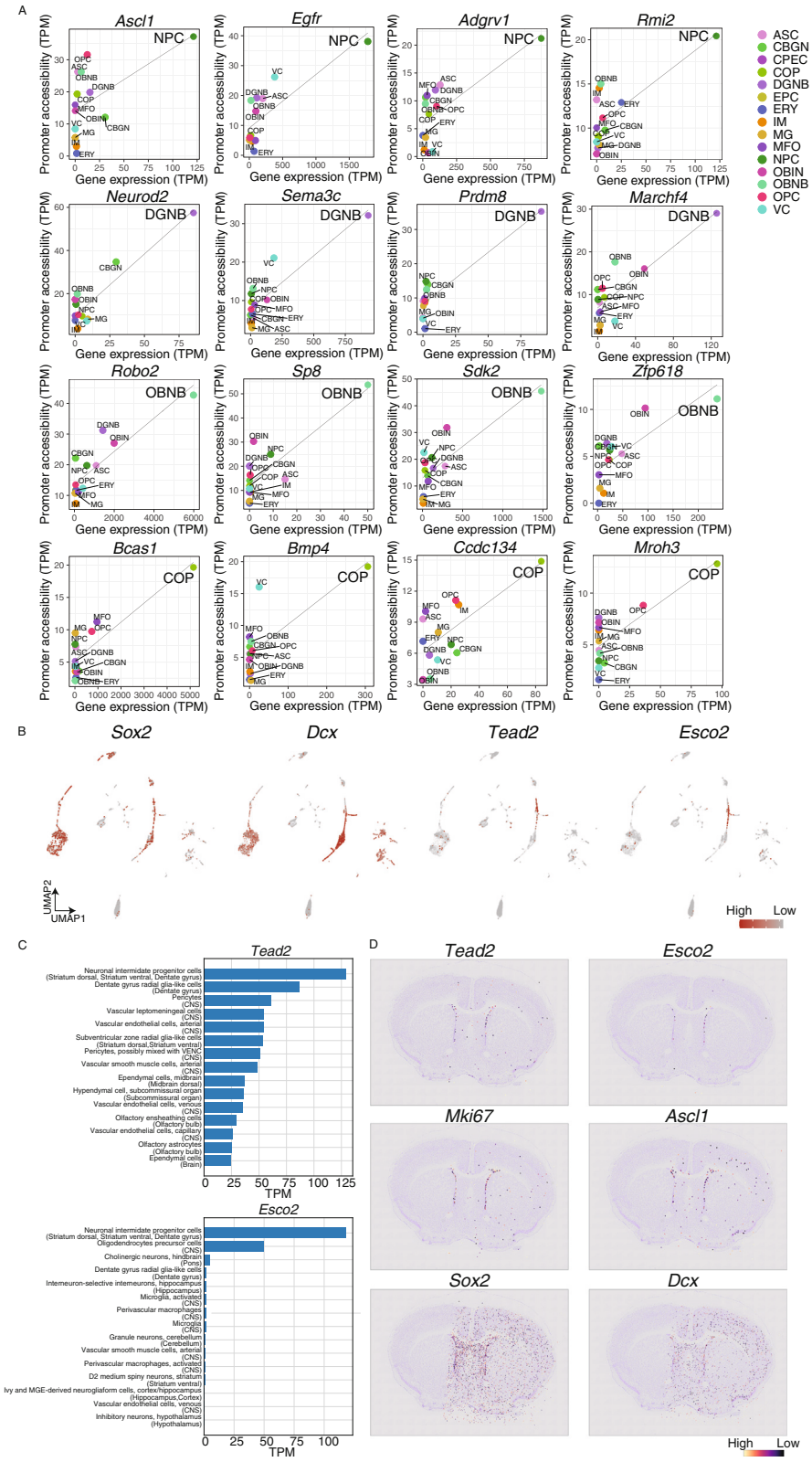

(legend on next page)

Figure S2. Identifying gene markers of neuronal progenitors and oligodendrocyte precursors, related to Figure 3

(A) Each scatterplot shows the correlation between expression and promoter accessibility of known (left two columns) or less-studied (right two columns) cell-type-specific gene markers, together with a linear regression line.

(B) UMAP plots showing the expression of two canonical neurogenesis markers, *Sox2* and *Dcx*, and two new markers, *Tead2* and *Esco2*, with higher specificity detected in our study.

(C) Bar plot showing the aggregated TPM (transcripts per million) of *Tead2* and *Esco2* among the top 15 expressed clusters from a published mouse brain atlas[26] with the anatomical region annotated. Both genes are topped in neuronal intermediate progenitor cells.

(D) Mouse coronal sections showing the normalized counts of *Tead2*, *Esco2*, *Ascl1*, *Mki67*, *Sox2*, and *Dcx* per bead using Slide-seq data from Langlieb et al.[27] Arrows indicate the subventricular zone where both *Tead2* and *Esco2* were detected, similar to the neuronal stem and progenitor cell marker *Mki67* and *Ascl1*.

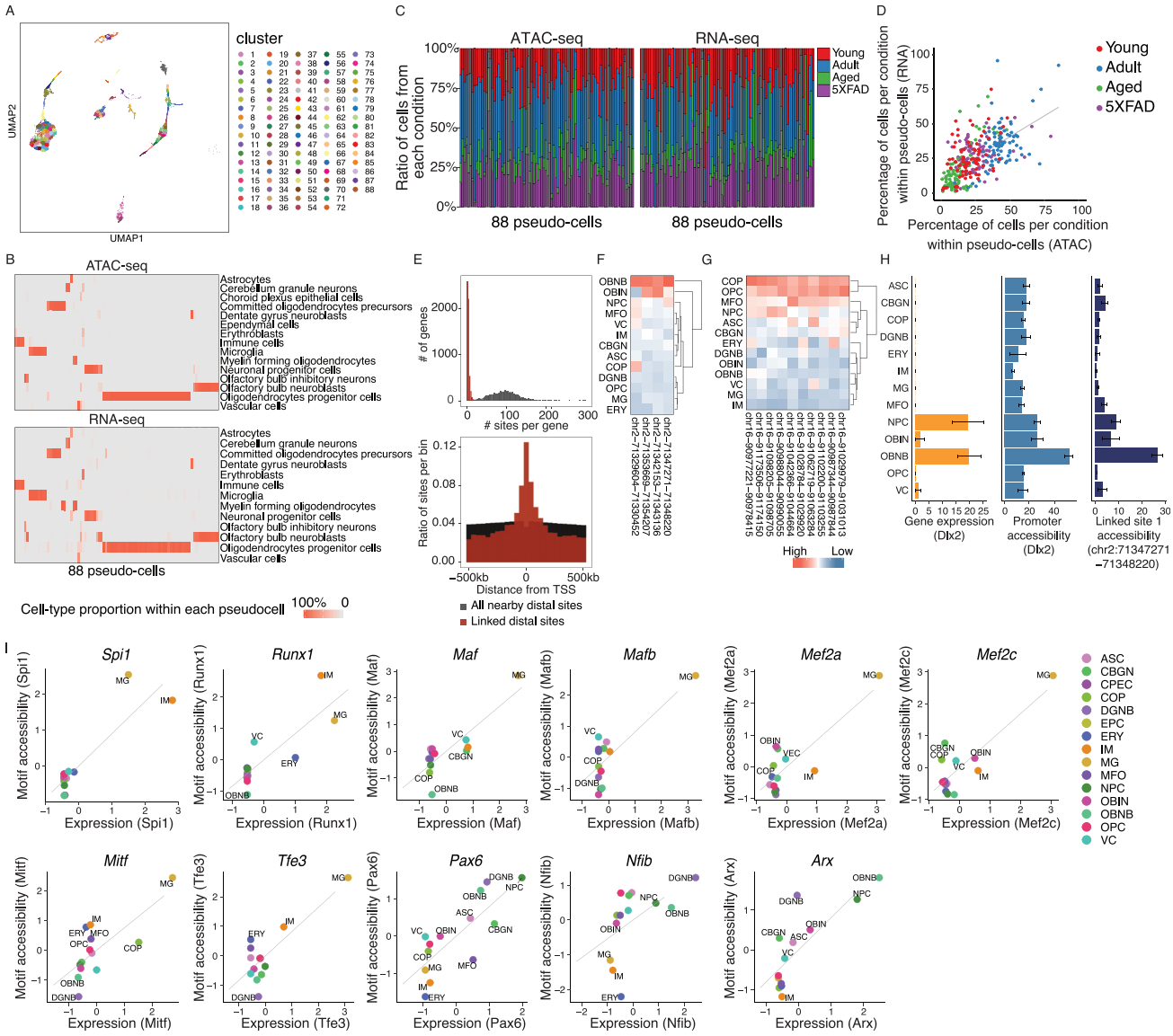

Figure S3. Linking *cis*-regulatory elements to their regulated genes and identifying key TF regulators, related to Figure 3

(A) UMAP visualization of EdU+ cells as in Figures 1D and 1E, colored by k-means clustering ID.

(B) Heatmap showing the ratio of cells from each cell type within each pseudo-cell.

(C) Stacked bar plot showing the ratio of cells from each condition within each pseudo-cell.

(D) Scatterplot showing the correlation in the cell fraction within each condition from ATAC-seq and RNA-seq per pseudo-cell.

(E) The left histogram shows the number of accessible sites per gene. The right histogram shows the distance distribution of accessible sites within 500 kb of genes. Both plots include all nearby accessible sites (colored in black) and the linked accessible sites (colored in red).

(F) Heatmap showing the cell-type-specific peak accessibility of four *Dlx2* linked sites. Cell types are ordered by hierarchical clustering.

(G) Heatmap showing the cell-type-specific peak accessibility of ten *Olig2* linked sites. Cell types are ordered by hierarchical clustering.

(H) Bar plots showing the average expression, the accessibility of promoter, and linked distal sites for neurogenesis marker *Dlx2* across different cell types. Gene expression values for each cell type were quantified by TPM. Site accessibilities for each cell were quantified by the number of reads per million. Error bars represent SEMs.

(I) Each scatterplot shows the correlation between cell-type-specific gene expression and motif accessibility for known TF regulators, together with a linear regression line.

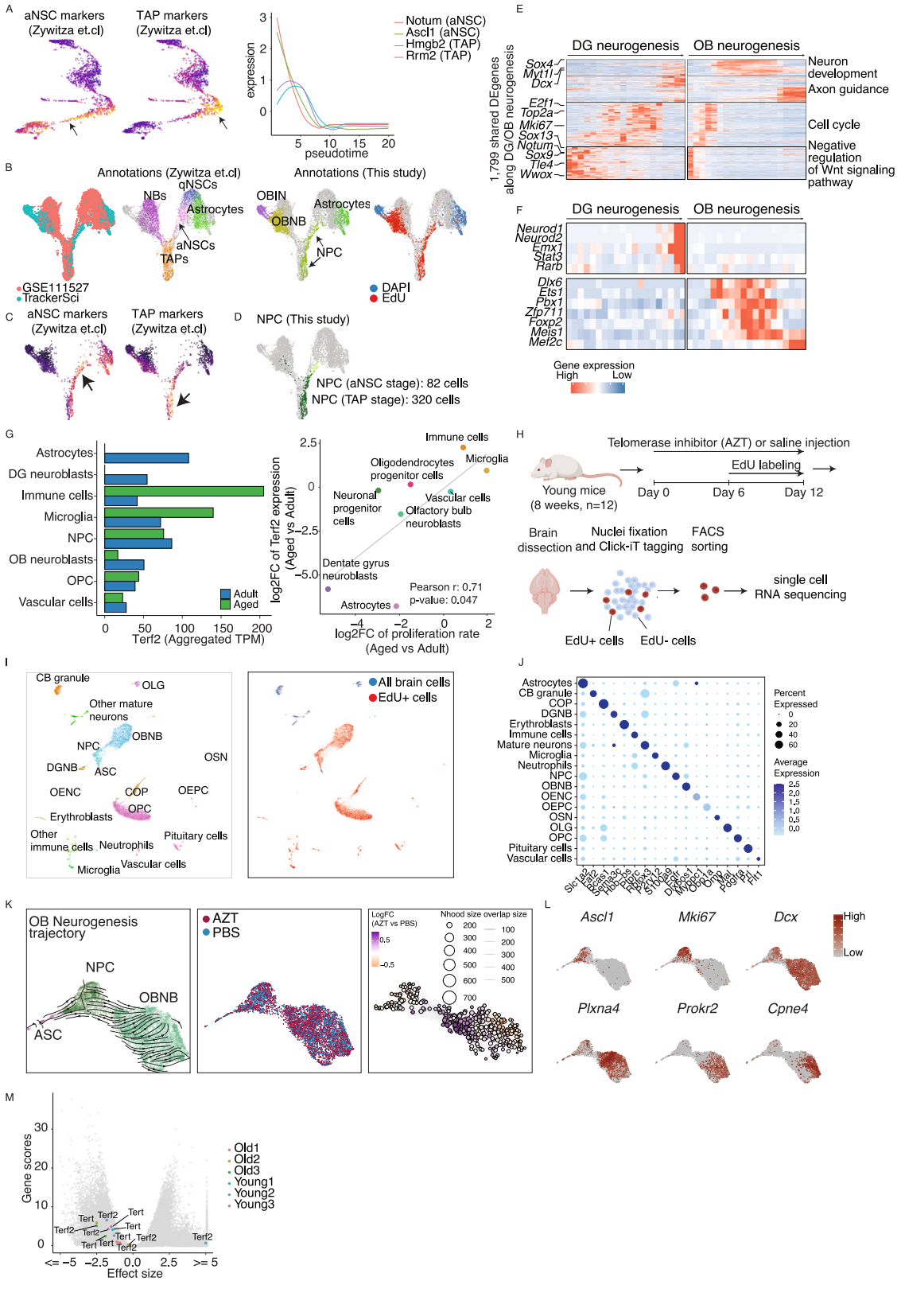

(legend on next page)

Figure S4. Characterizing adult neurogenesis and functionally examining the impact of telomere and telomerase activity on it through *in vivo* drug treatment, related to Figure 5

(A) Left: UMAP plots showing the activated neuronal stem cell (aNSC) gene markers and transient amplifying (TAP) gene markers along the neurogenesis trajectory. Arrows indicate the aNSC stage and TAP stage. Right: expression dynamics of representative aNSC marker (*Notum* and *Ascl1*) and TAP markers (*Hmgb2* and *Rrm2*) along differentiation pseudotime of the neurogenesis trajectory depicted in Figure 5A.

(B) UMAP plot showing integrated cells between *TrackerSci* dataset and the published SVZ dataset from Zywitza et al.,[39] colored by data source, published cell annotation, *TrackerSci* annotation, and *TrackerSci* assay type. Only OB neurogenesis-related cells were used from the *TrackerSci* dataset.

(C) UMAP plots showing aNSC gene markers and TAP gene markers along the integrated trajectory.

(D) UMAP plot highlighting NPCs from *TrackerSci*, colored by sub-stage annotation.

€ Heatmap showing the dynamics of gene expression of 1,799 shared DE genes along DG neurogenesis (left) and OB neurogenesis (right). Genes are ordered and clustered by hierarchical clustering. Representative gene names (left) and enriched pathways (right) for each gene group are labeled.

(F) Heatmap showing example TFs exhibiting trajectory-specific gene expression dynamics: *Neurod1*, *Neurod2*, *Emx1*, *Stat3*, and *Rarb* are uniquely upregulated in DG neurogenesis, while *Dlx6*, *Ets1*, *Pbx1*, *Zfp711*, *Foxp2*, *Meis1*, and *Mef2c* are uniquely upregulated in OB neurogenesis.

(G) Left: a bar plot showing the aggregated expression (TPM) of *Terf2* across different progenitor cell types in adult or aged mouse brains. Right: a scatterplot elucidating the correlation between alterations in *Terf2* expression and cell-type-specific proliferation rates between aged and adult brains.

(H) A schematic of the experimental design for *TrackerSci* analysis of cell dynamics following AZT treatment.

(I) UMAP visualization of cells retrieved from the drug treatment experiment, distinguished by primary cell types (left) and source (right). ASC, astrocyte; COP, committed oligodendrocyte precursor; DGNB, dentate gyrus neuroblast; OLG, oligodendrocyte; NPC, neuronal progenitor cell; OBNB, olfactory bulb neuroblast; OENC, olfactory ensheathing cell; OEPC, olfactory epithelial cell; OSN, olfactory sensory neuron; OPC, oligodendrocyte progenitor cell.

(J) A dot plot demonstrating the expression of marker genes across main cell types.

(K) UMAP plots of OB neurogenesis cells, categorized by primary cell types with cell transition direction inferred from RNA velocity analysis (left) and by condition (middle). On the right, a neighborhood graph from the Milo differential abundance analysis[50] on the OB neurogenesis trajectory is shown. Nodes symbolize cellular neighborhoods from the KNN graph, colored by the log-transformed fold change before and after AZT treatment. Graph edges represent the number of cells shared between neighborhoods.

(L) UMAP plots exhibiting the expression of representative stage-specific genes, including the aNSC marker *Ascl1*, TAP cell marker *Mki67*, pan-immature neuron marker *Dcx*, and other representative genes with transient expression along the trajectory (*Plxna4*, *Prokr2*, and *Cpne4*).[124,125]

(M) Volcano plots showing CRISPR screen results from Ruetz et al.,[54] highlighting knocking out *Terf2* or *Tert* impeding primary NSC proliferation (depleted gRNAs), colored by the origin of cells from replicates.

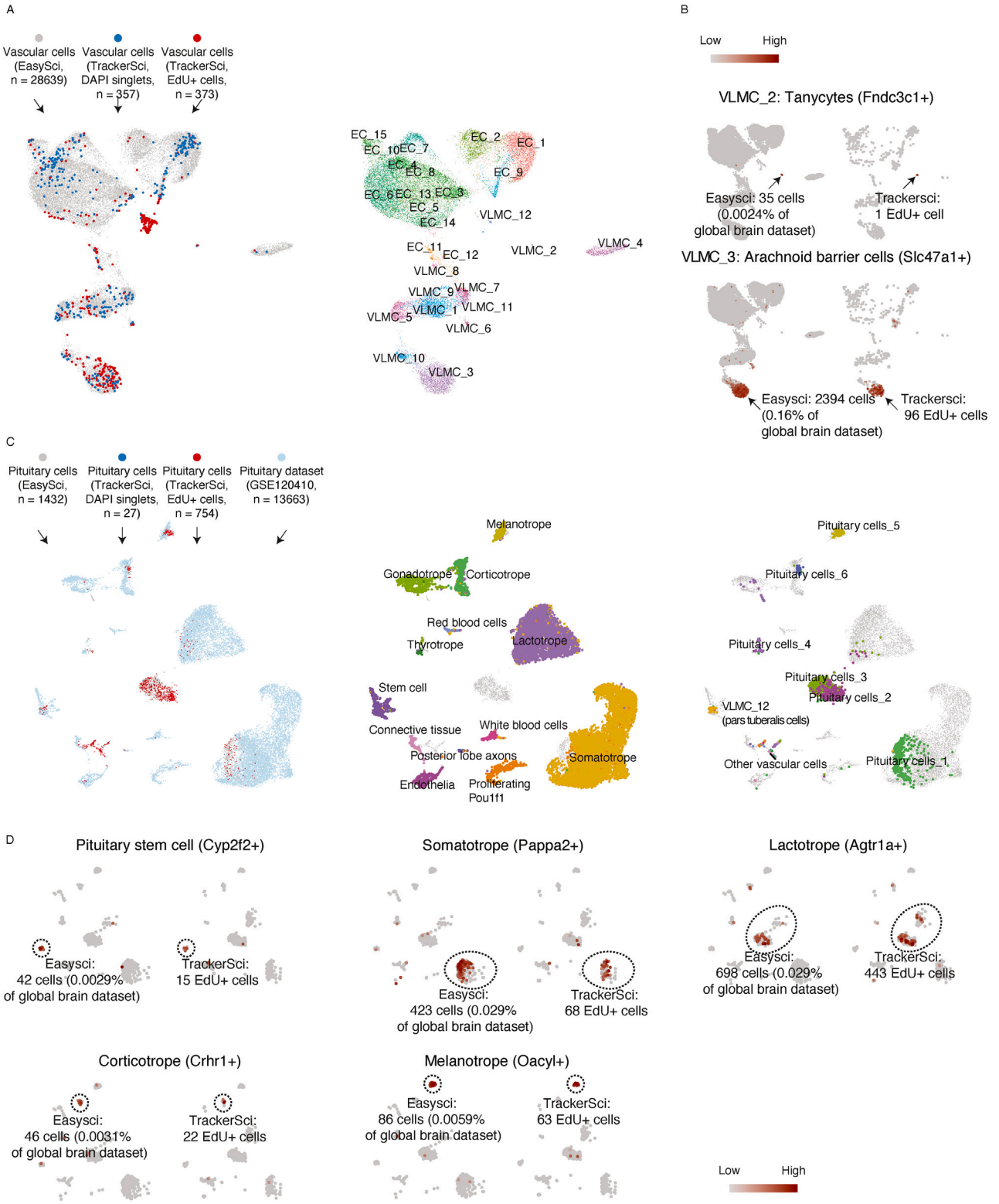

(legend on next page)

Figure S5. Identification of proliferating arachnoid barrier cells and pituitary cells in the mouse brain, related to Figure 5

(A) UMAP plots showing the integrated vascular cells colored by assay types (left) and subcluster ID from the *EasySci* brain cell atlas (right).

(B) UMAP plots showing the expression of tanycytes marker *Fndc3c1*[126] (top) and arachnoid barrier cells marker *Slc47a1*[64] (bottom) in the *EasySci* dataset (left) and *TrackerSci* dataset (right).

(C) UMAP plots showing the integrated pituitary cells colored by assay types (left), cell annotation from the published study,[65] and subcluster ID from the *EasySci* brain cell atlas[15] (right).

(D) UMAP plots showing the expression of pituitary stem cell marker *Cyp2f2*,[65] somatotrope marker *Pappa2*,[65] lactotrope marker *Agtr1a*,[65] corticotrope marker *Crhr1*,[65] and melanotrope marker *Oacyl*[65] in the *EasySci* dataset (left) and *TrackerSci* dataset (right). Gene expression values were calculated by normalizing the UMI count matrix to the library size and then log transformed and scaled.

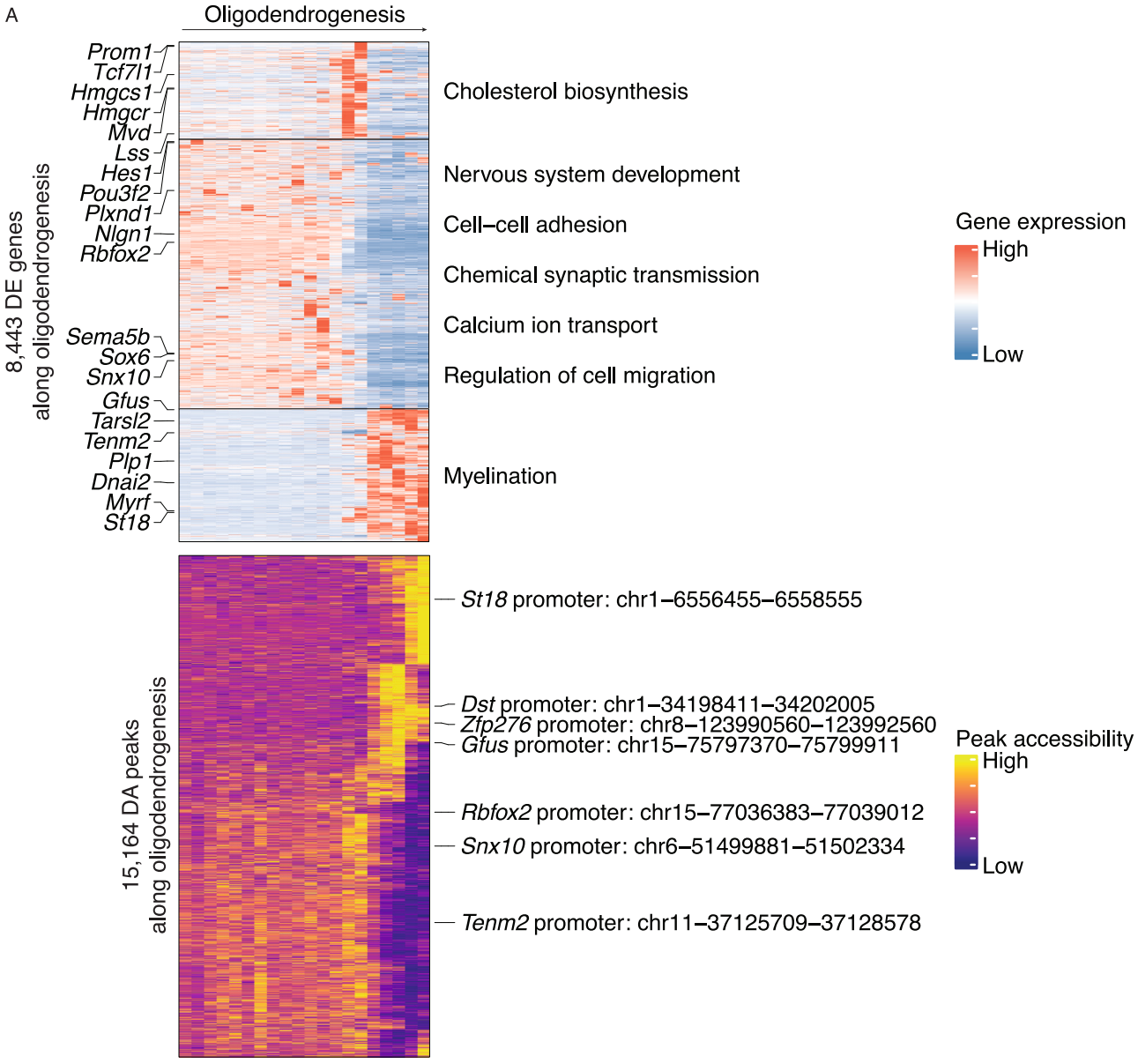

(legend on next page)

Figure S6. Characterization of adult oligodendrogenesis and increased expression of *C4b* in OPCs during aging, related to Figure 6

(A) Heatmap showing the dynamics of 8,443 DE genes (top) and 15,164 DA sites (bottom) along the oligodendrogenesis trajectory. Genes are ordered and clustered based on hierarchical clustering. Representative gene names (left) and enriched pathways (right) for each gene group are labeled. Peaks are ordered based on hierarchical clustering, and peaks corresponding to promoters of oligodendrogenesis markers are labeled.

(B) Bar plots showing the gene expression (left) and promoter accessibility (middle) of *C4b* from the *TrackerSci* dataset and the gene expression of *C4b* from the *EasySci* dataset (right) in OPCs and COPs, quantified by TPM for gene expression and reads per million for promoter accessibility. Error bars represent SEMs.

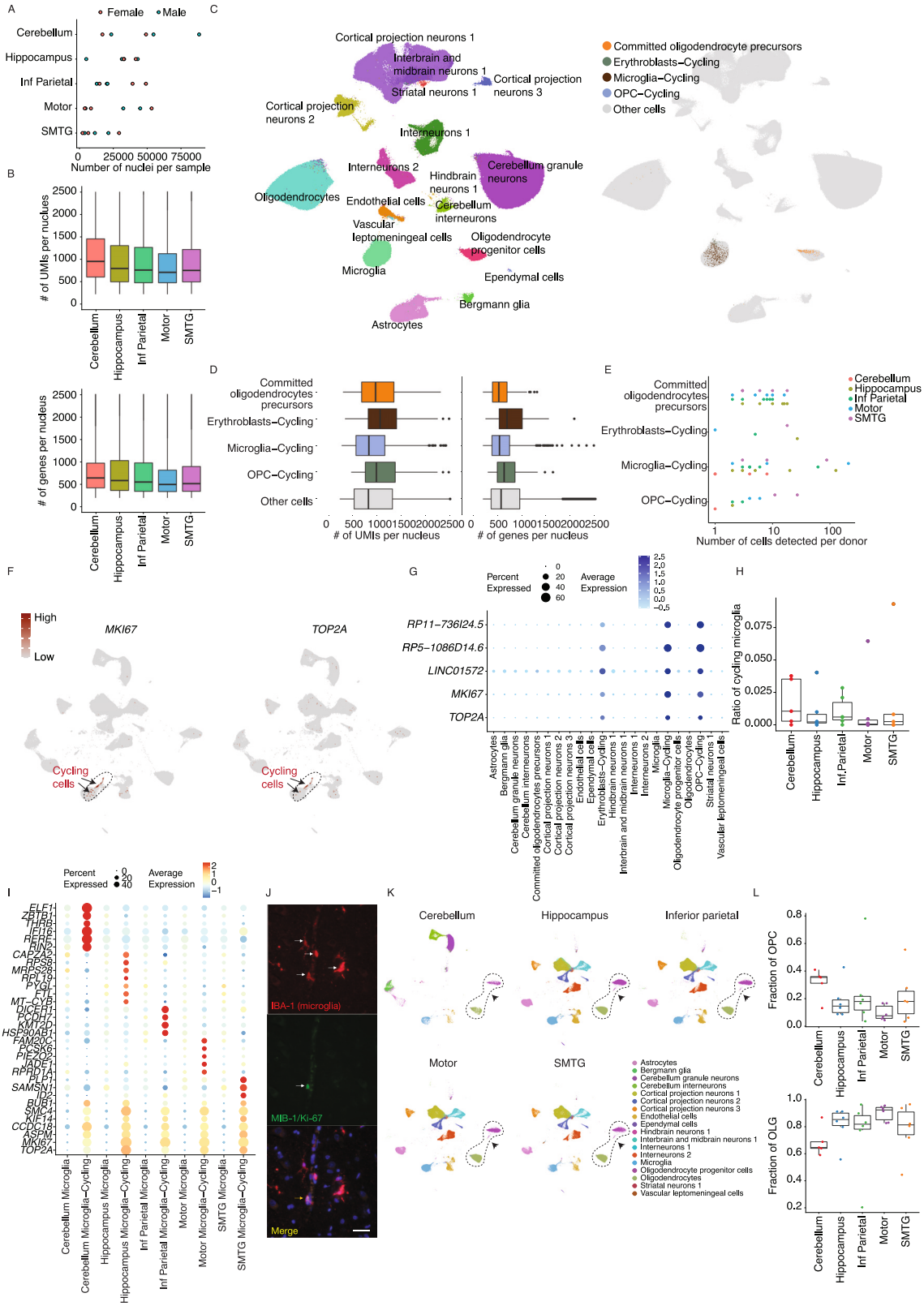

(legend on next page)

Figure S7. Quality control and characterization of rare proliferating and differentiating cells in the human brain dataset, related to Figure 7

(A) Scatterplot showing the number of single-cell transcriptomes profiled in each human sample across five regions, colored by sexes.

(B) Boxplots showing the number of unique transcripts (left) and genes (right) detected per nucleus profiled by *EasySci* in the human dataset. For all boxplots: middle lines, medians; upper and lower box edges, first and third quartiles, respectively; whiskers, 1.5 times the interquartile range; and circles are outliers.

(C) UMAP visualization of the full human brain dataset (~800,000 cells) with the same parameter settings as in Figure 7A, colored by main cell types (left) and cycling and differentiating cells (right). Note that rare cycling and differentiating cells are masked in the main clustering analysis.

(D) Boxplots showing the number of unique transcripts (left) and genes (right) detected per nucleus comparing the rare proliferating and differentiating cells and the rest of cells.

(E) Dot plot showing the number of nuclei captured per donor for each rare proliferating or differentiating subtype, colored by the source of the region.

(F) UMAP plots showing the expression of proliferating markers *MKI67* (left) and *TOP2A* (right) across the entire dataset. The single-cell expression data (UMI count) were normalized first by the total number of reads for each cell and then log transformed and scaled.

(G) Dot plot showing the markers for cycling cells, including noncoding RNA (*RP11-736I24.5*, *RP5-1086D14.6*, and *LINC01572*) and canonical cycling markers (*MKI67* and *TOP2A*).

(H) Boxplot showing the fraction of cycling microglia to the rest of microglia cells across different brain regions in each sample.

(I) Dot plot showing examples of region-specific and shared gene expression signatures for cycling microglia across brain regions.

(J) Representative fluorescence microscopy images of human brain tissue, staining for microglia marker (IBA1+) and proliferation marker (KI67+); nuclei stained with blue DAPI. The arrow indicates a proliferating microglia IBA1/KI67+ among the IBA1+ microglia cells. Scale bars, 50 μm.

(K) UMAP plot same as in Figure 7A split by five brain regions colored by main cell types, indicating the loss of intermediate oligodendrogenesis cells in the cerebrum.

(L) Boxplot showing the fraction of OPCs (top) and mature oligodendrocytes (OLGs, bottom) among oligodendrogenesis-related cells across different brain regions in each sample.

(legend on next page)

Figure S8. Detection of immature hippocampus neurons, cycling microglia, and COPs in the external human brain datasets through integration analysis, related to Figure 7

(A) UMAP plots showing the integrated cells across the published human brain dataset,[86] the *EasySci* human brain dataset, and the *TrackerSci* mouse brain dataset, colored by the data source (upper left), cell annotations from the published human dataset (upper right), cell annotations from the *TrackerSci* mouse dataset (lower left), or cell annotations from the *EasySci* human dataset (lower right). Cells from other datasets are colored in gray. The arrow indicates the immature neuron population. ASC, astrocyte; BG, Bergmann glia; CBGN, cerebellum granule neuron; CBIN, cerebellum inhibitory neuron; COP, committed oligodendrocyte precursor; CPN1, cortical projection neuron 1; CPN2, cortical projection neuron 2; CPN3, cortical projection neuron 3; DGNB, dentate gyrus neuroblast; EC, endothelial cell; EPC, ependymal cell; HN1, hindbrain neuron 1; IMN1, interbrain and midbrain neuron 1; IN1, interneuron 1; IN2, interneuron 2; MG, microglia; NPC, neuronal progenitor cell; OBNB, olfactory bulb neuroblast; OBIN, olfactory bulb inhibitory neuron; OPC, oligodendrocyte progenitor cell; OLG, oligodendrocyte; SN1, striatal neuron 1; VLEC, vascular leptomeningeal cell.

(B) UMAP plots showing the enriched expression of *SOX4* (left) and *SOX11* (right) within immature neuron cells, conserved between human hippocampus cells from the published dataset (top) and the mouse cells from the *TrackerSci* dataset (bottom).

(C) UMAP plots showing the integrated cells across the published human AD brain dataset,[90] the *EasySci* human brain dataset, and the *TrackerSci* mouse brain dataset, colored by the data source (left, cells from *TrackerSci* are annotated), cell annotations from the *EasySci* human dataset (middle, cells from other datasets colored in gray), or cell annotations from the published human AD dataset (right, cells from other datasets colored in gray). The arrow indicates the cycling or progenitor cells in three datasets.

(D) UMAP plots showing the expression of COP genes *GPR17* (left) and *SIRT2* (right).

(E) UMAP plots showing the expression of proliferation marker genes *MKI67* (left), *TOP2A* (middle), and microglia marker *CSF1R* (right). The arrow indicates the proliferating microglia.

(F) UMAP plots zooming into the microglia-related cells, split by AD brain cells (left) and control cells (right).

(G) Boxplot comparing the ratio of proliferating microglia among all microglia between AD and control samples in two brain regions. Numbers represent the p values using the Wilcoxon rank-sum test.